COMPARISON OF Cd^{2+} BIOSORPTION AND BIOACCUMULATION BY BACTERIA – A RADIOMETRIC STUDY

LINDA MACHALOVÁ, MARTIN PIPÍŠKA, ZUZANA TRAJTEĽOVÁ, MIROSLAV HORNÍK

Department of Ecochemistry and Radioecology, University of SS. Cyril and Methodius, J. Herdu 2, Trnava, SK-917 01, Slovak Republic (martin.pipiska@ucm.sk)

Abstract: In this work, bioaccumulation and biosorption characteristics of Cd^{2+} ions by both dead and living non-growing biomass of gram-positive bacteria *Kocuria palustris* and *Micrococcus luteus* isolated from spent nuclear fuel pools were compared. The radioindicator method with radionuclide ^{109}Cd was used to obtain precise and reliable data characterizing Cd compartmentalization in bacterial cells. The following cellular distribution of Cd in living non-growing biomass after 4 h incubation in solutions containing different concentration of Cd^{2+} ions (100, 250, 500, 750 and 1000 μmol/L) spiked with $^{109}CdCl_2$ under aeration at 30 °C were obtained: in *M. luteus* almost 85 % of Cd was localized on the cell surface and 15 % in cytoplasm. Similarly, in *K. palustris* 83 % of Cd was localized on the cell surface and 17 % in cytoplasm. The data were obtained by gamma spectrometry of extracts and solids after sequential extraction of biomass with 5 mM $Ca(NO_3)_2$ and 20 mM EDTA. Biosorption of Cd by non-living bacterial biomass is a rapid process strongly affected by solution pH and as was confirmed by FTIR analysis beside carboxylate ions also other functional groups such as amino and phosphate contribute to Cd binding by bacterial cell surfaces. Maximum sorption capacities Q_{max} (μmol/g) calculated from the Langmuir isotherm were 444 ± 15 μmol/g for *M. luteus* and 381 ± 1 μmol/g for *K. palustris*.

Key words: ^{109}Cd, bioaccumulation, biosorption, *Micrococcus, Kocuria*,

1. Introduction

Rapid industrialization and urbanization have resulted in the generation of large quantities of aqueous effluents, many of which contain high level of toxic pollutants such as heavy metals, organic compounds and radionuclides (REMENÁROVÁ *et al*., 2012). From current research activities is evident that various technologies based on interactions between pollutants and biological systems in a contaminated environment are investigated (CHOJNACKA, 2010; SINGH and TRIPATHI, 2007). Biosorption and bioaccumulation have been investigated as promising processes of toxic metal removal. Such processes appear as ideal candidates for replacing conventional methods for metal removal from wastewaters such as chemical precipitation, electrowinning, membrane separation, evaporation and ion-exchange, especially in cases when low concentrations of metals are present in wastewaters (REMENÁROVÁ *et al.,* 2012).

Biosorption is a surface phenomenon where one or more physico-chemical mechanisms are involved in metal uptake by both dead and living biomass. However, bioaccumulation is an intracellular metabolically dependent metal accumulation and involves metal binding on intracellular compounds, intracellular precipitation, methylation and other mechanisms. Bioaccumulation can also be regarded as a second

DOI 10.1515/nbec-2015-0024

part of the metal sequestering process by living biomass (KADUKOVÁ and VIRČÍKOVÁ, 2005). CAMBEL *et al.* (2002) stated that the formation of complexes between metals and anionic functional groups on cell surfaces is viewed as a pre-requisite for uptake of metals by the organism. Once surface sorption occurs, the metal may be transported into the cytoplasm.

Both processes can be considered as two major biological techniques for the removal of toxic metals. From this point of view the increased interest of microorganisms application in metal sequestration was recently observed (CHOJNACKA, 2007). However, only a few experimental studies dealing with comparison of metal biosorption and bioaccumulation by microrganisms can be found. KADUKOVÁ and VIRČÍKOVÁ (2005) revealed that the Cu binding capacity of living cells of algae *Chlorella kessleri* is significantly lower than the capacity of dead cells. On the contrary VARGAS-GARCÍA *et al.* (2012) observed that fungi isolated from compost showed a higher efficiency against Cd, Pb, Ni, Cr, Zn and the predominant removal mechanism was intracellular accumulation, which made growing cells more efficient than dead biomass as detoxifying agents. Also uptake of the thallium by fungus *Neosartorya fischeri* is highly enhanced when the active biomass is used (URÍK *et al*., 2010). ALAM and AHMAD (2013) found that biosorption of Cd^{2+}, Ni^{2+}, Cu^{2+} and Zn^{2+} ions was higher with the non-growing biomass of bacteria *Exiguobacterium* sp. ZM-2 compared to the dried biomass. It is evident that discussion whether to employ the living or dead cells for bioremediation still take place in literature.

The objectives of the present study were to determine effects of Cd^{2+} ions on growth of Gram-positive bacteria *Kocuria palustris* and *Micrococcus luteus* isolated from spent nuclear fuel pools and to investigate the differences between Cd^{2+} ions biosorption and bioaccumulation by dead and live non-growing bacteria. The radioindicator method with radionuclide ^{109}Cd was used to obtain precise and reliable data characterizing Cd compartmentalization in bacterial cells.

2. Material and methods

2.1 Bacteria isolation and cultivation

Gram-positive bacteria were isolated from pool water in the Interim Spent Nuclear Fuel Storage Facility in JAVYS a.s. in Jaslovské Bohunice, Slovak Republic. Isolates were further identified using 16S rDNA methods as *Kocuria palustris* and *Micrococcus luteus* (TIŠÁKOVÁ *et al*., 2013). Bacteria were grown on DEV nutrient agar at 22 ± 2°C (Merck, Germany) and maintained at 4°C.

Bacteria were cultivated in nutrient broth (peptone 10 g/L, beef extract 10 g/L, NaCl 5 g/L, pH 7.4 ± 0.2) on a rotary shaker (Biosan ES 20) for 24 - 32 h at 30 °C. Subsequently, cells were harvested at stationary phase by centrifugation (4500 rpm, 5 min) and rinsed two times with deionized water. Such bacterial pellet was used in bioaccumulation experiments. Bacterial pellet was also dried for 24 h at a maximum of 60°C to avoid the degradation of binding sites. Dried biomass was crushed into a fine powder, sieved and used in biosorption experiments.

2.2 Inhibition activity

A micro dilution method was performed in 96-well sterile microplates to determine inhibition activity and ID_{50} values of Cd^{2+} ions for *K. palustris* and *M. luteus*. Briefly, 100 µL of steriled deionized water was added to each well. To wells in column 1 was added 100 µL of $CdCl_2$ solution (4 mmol/L) and mixed well with a micropipette. Subsequently, 100 µL of solution from column 1 was transferred into column 2 yielding two-fold serial dilution. Procedure was repeated down to column 12. Actively growing bacteria (100 µl) from subculture was added to each of the wells except the row 1 which serves as control. The microplate was placed on rotary shaker (30 °C, 140 rpm) and cultivated for 48 h. In time intervals, the optical density (OD) was measured at λ= 600 nm using microplate reader ELx800 (BioTek, USA).

Suspensions of *M. luteus* or *K. palustris* were prepared from 72 h subculture in fresh nutrient medium (10 g peptone, 10 g beef extract, 5 g NaCl per liter). Subculture (5 ml) was put into 30 ml of fresh nutrient broth and placed on rotary shaker (30°C, 140 rpm) for 30 min.

2.3 Bioaccumulation and cell compartmentalization of Cd^{2+} ions

Living bacterial cells harvested from stationary phase (see section 2.1) were added to 10 mL of Cd solution (100 µmol/L $CdCl_2$, pH 6.0) spiked with ^{109}Cd (37.1 kBq/L) in Erlenmayer flasks. Flasks were shaken at 150 rpm (rotary shaker Biosan ES 20) at 25°C for 4 h. In time intervals the content of the flasks was centrifuged (4 500 rpm, 4 min), bacterial pellet was washed in deionized water and radioactivity of cells was measured using scintillation gamma-spectrometry. Biomass dry weight was estimated after drying for 24 h at 60 °C. Cadmium uptake was calculated according to (1):

$$Q = (C_0 - C_f)\frac{V}{M} \quad (1)$$

where Q is the Cd uptake (µmol/g), C_0 and C_f are the initial and the final Cd concentrations in solution (µmol/L), V is volume (L) and M is the amount of bacterial biomass (d.w.; given in grams).

Similarly, living bacterial cells harvested from stationary phase were added to 10 mL of Cd solution with initial concentration C_0 = 100, 250, 500, 750, 1000 µmol/L of $CdCl_2$ labelled with ^{109}Cd (37.1 kBq/L) in Erlenmayer flasks and pH was adjusted to 6.0. Flasks were shaken at 150 rpm at 25°C. After 1 h the content of the flasks was centrifuged (4 500 rpm, 4 min), bacterial pellet was washed in deionized water and radioactivity of cells was measured. Biomass dry weight was estimated after drying for 24 h at 60 °C. Metal uptake was calculated according to equation (1).

Cell compartmentalization of Cd was determined using modified sequential extraction procedure according to PABST *et al.* (2010) and HUANG *et al.* (2014). Metals associated with exchange sites on the cell surface were extracted by resuspending the cell pellet in 10 mL of 5 mM $Ca(NO_3)_2$ for 15 min with gentle shaking at 40 rpm. The suspension was centrifuged (4 500 rpm) and the radioactivity of cells was measured. Subsequently, the cell pellet was treated with 10 mL of 20 mM

EDTA (tetrasodium salt dehydrate) for 1 min to solubilise. The EDTA remove Cd tightly bound to cell surface. After centrifugation (4 500 rpm, 4 min) supernatant radioactivity was measured. The radioactivity of remaining pellet was also measured and represents intracellularly localized Cd. All tubes with biomass were weight between extraction steps and at the end of experiments dried to constant weight. Cadmium uptake was calculated according to (1). All experiments were performed in duplicate series.

The Langmuir model (see below) was used to analyse the distribution of Cd associated with cell compartments of *K. palustris* and *M. luteus*.

2.4 Biosorption kinetics

Dried biomass of *K. palustris* and *M. luteus* was added to 8 mL of Cd solution (1000 μmol/L $CdCl_2$, ^{109}Cd 58.1 kBq/L). Solution pH was adjusted to 6.0 and flasks were incubated on rotary shaker (150 rpm) at 25°C. At the time intervals 60, 120, 240, 360, 1440 min the content of the flask was centrifuged (4 500 rpm, 4 min) and the biomass radioactivity was measured. All experiments were performed in duplicate series. The cadmium uptake was calculated according to (1).

2.5 Biosorption equilibrium

Dried bacterial biomass was added to 8 mL of Cd solution with initial concentrations C_0 = 100, 500, 1000, 2000 and 4000 μmol/L $CdCl_2$ labelled with ^{109}Cd (37.1 kBq/L) and pH was adjusted to 6.0. Flasks were incubated on rotary shaker (150 rpm) at 25°C. After 4 h the content of the flasks was centrifuged (4 500 rpm, 4 min) and the biomass radioactivity was measured. All experiments were performed in duplicate series. The cadmium uptake was calculated according to (1).

Equilibrium data were analysed using adsorption Langmuir (2) and Freundlich (3) isotherm models.

$$Q_{eq} = \frac{bQ_{\max}C_{eq}}{1 + bC_{eq}} \tag{2}$$

$$Q_{eq} = KC_{eq}^{(1/n)} \tag{3}$$

where Q_{max} represents the maximum Cd sorption capacity of bacterial biomass, b is a constant related to the energy of sorption. K and $1/n$ values are the Freundlich constants referring to sorption capacity and intensity of sorption, respectively. To calculate the Q_{max} values and the corresponding parameters of isotherms non-linear regression analysis was performed by ORIGIN 7.0 Professional (OriginLab Corporation, Northampton, USA).

2.6 Effects of pH

To analyze the influence of pH, dried bacterial biomass was shaken in Cd^{2+} solutions (C_0 = 1000 μM) of desired pH spiked with ^{109}Cd (48.3 kBq/L) for 4 h on a

rotary shaker at 150 rpm and 25°C. In order to eliminate interference of buffer components on Cd biosorption, the non-buffered solutions in deionised water were adjusted to the desired pH values by adding 0.5 M HCl or 0.1 M NaOH.

2.7 Speciation modeling

Prediction of the speciation of cadmium in the aqueous systems as a function of total salt concentration and solution pH was performed using the Visual MINTEQ (version 3.0) program. Visual MINTEQ is a chemical equilibrium program that has an extensive thermodynamic database for the calculation of metal speciation, solubility and equilibria (GUSTAFFSON, 2004). All data sets were calculated considering the carbonate system naturally in equilibrium with atmospheric CO_2 (pCO_2 = 38.5 Pa).

2.8 Radiometric analysis

The gamma spectrometric assembly using the well type scintillation detector 54BP54/2-X, NaI(Tl) (Scionix, the Netherlands) and the data processing software Scintivision 32 (ORTEC, USA) were used for ^{109}Cd determination at the energy of γ-photons ^{109}Cd – 88.04 keV. Standardized $^{109}CdCl_2$ solution (3.857 MBq/mL, $CdCl_2$ 50 mg/L in 3 g/L HCl) was obtained from the Czech Institute of Metrology, Prague (Czech Republic).

2.9 FTIR analysis

FTIR analysis was carried out to identify chemical functional groups on dried bacterial biomass and to explain the Cd biosorption mechanism. FTIR analysis was performed by Affinity 1 spectrometer (SHIMADZU, Japan). Samples of dried *K. palustris* and *M. luteus* biomass before and after Cd biosorption (C_0 = 4 mM $CdCl_2$; pH 6.0; 4 h) were mixed with KBr at a ratio 1:100 for making pellets and the FTIR spectra were obtained within the range 400-4000 cm^{-1}.

3. Results and discussion

3.1 Effect of Cd^{2+} ions on bacterial growth

The toxic effects of an increasing concentration of Cd^{2+} ions on the growth of G+ bacteria *K. palustris* and *M. luteus,* isolated from deionized water in Interim Spent Nuclear Fuel Facility in JAVYS a.s., Jaslovské Bohunice, Slovak Republic (TIŠÁKOVÁ *et al.*, 2013), were studied using the microplate dilution method. 3D diagrams of bacterial growth curves in the presence of various Cd^{2+} ions concentrations in cultivation medium are shown on Fig. 1A, B. Such representation helps finding detailed description of the growth difference between *K. palustris* and *M. luteus*. Without the presence of Cd^{2+} ions both species showed logarithmic growth during the majority of the incubation time (not shown). Both bacteria were able to grow at 0.063 mM $CdCl_2$, while concentrations from 0.125 to 2 mM were highly toxic

and significantly inhibited the bacterial growth in comparison with growth of control culture.

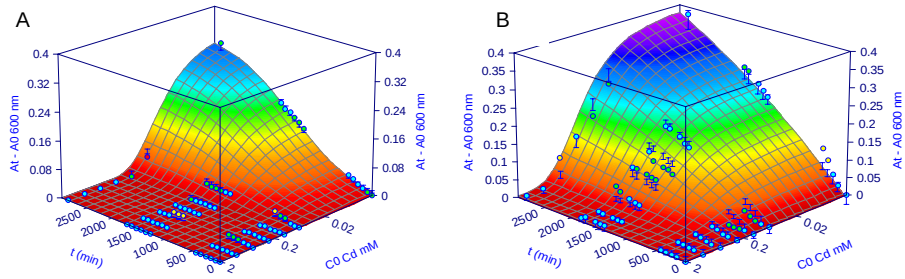

Fig. 1. 3D diagrams of growth curves of bacteria *Kocuria palustris* (A) and *Micrococcus luteus* (B) in nutrient broth with Cd^{2+} ions. The X-axis is the Cd^{2+} concentration (0.063 – 2 mM $CdCl_2$) in medium, the Y-axis is the incubation time and the Z-axis is the optical density measured at λ = 600 nm. Cultivation in microplate on rotary shaker (140 rpm) at 30°C. $A_0 = 0.122 \pm 0.008$ (*K. palustris*) and $A_0 = 0.100 \pm 0.003$ (*M. luteus*). Individual points represent mean (n = 3). Points represent experimental data of absorbance ($A_t - A_0$).

In case of *K. palustris*, the long *lag* phase was observed at 0.125 mM $CdCl_2$, while cadmium concentrations from 0.25 to 2 mM fully inhibited the bacterial growth (Fig. 1A). From Fig. 2B it is evident that Cd concentrations from 0.125 to 0.5 mM reduced the *lag* phase and *M. luteus* grew slowly during a studied cultivation period. Almost complete growth inhibition of *M. luteus* was observed at concentrations 1 and 2 mM $CdCl_2$, respectively. Similarly, the major elongation of *lag* phase of *Bacillus cereus* RC-1 under higher cadmium concentrations was observed by HUANG *et al.* (2014).

The inhibition concentration IC_{50} values (mM) of Cd obtained after 48 h cultivation are shown in Table 1. Cd IC_{50} for *M. luteus* was 5 times higher than the IC_{50} for *K. palustris* indicating slightly higher resistance of *M. lutues* toward Cd ions. IC_{50} values of Cd for both isolates are comparable with IC_{50} for *E. coli* (ADAM *et al*., 2014) and significantly lower in comparison with Cd IC_{50} values for *Stenotrophomonas sp*. and *Ochrobactrum sp*. isolated from metal acclimatized activated sludge (BESTAWY *et al*., 2013).

Table 1. Inhibition of bacterial growth by $CdCl_2$ as IC_{50} (mM) concentrations after 48 h cultivation at 30 °C. Experimental data see in Fig. 1.

Bacteria	**IC_{50} (mM)**	**References**
Kocuria palustris	0.02	this work
Micrococcus luteus	0.10	this work
Escherichia coli NCTC 13216	0.04	ADAM *et al*. (2014)
Stenotrophomonas sp.	2.8	BESTAWY *et al*. (2013)
Ochrobactrum sp.	1.3	BESTAWY *et al*. (2013)

3.2 Cd^{2+} uptake by living bacteria

When living bacteria are used for metal removal the uptake process consists of metabolism independent extracellular binding (biosorption) and metabolism dependent

intracellular uptake (bioaccumulation). To obtain precise quantitative data characterizing the location of Cd in bacterial cell compartments a radioindicator method with radionuclide ^{109}Cd was used in our experiments. At the pH 6.0, Cd was present in solutions predominantly as the free ions Cd^{2+} (87.5 %) and as a complex $CdCl^{+}$ (12.6 %) (determined by Visual MINTEQ speciation program).

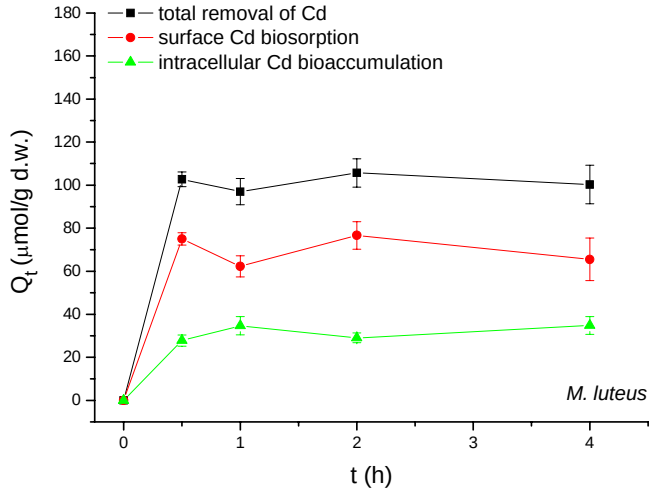

Fig. 2. Kinetics of Cd removal (C_0 = 100 µmol/L $CdCl_2$, 37.1 kBq/L $^{109}CdCl_2$) by living non-growing cells of *M. luteus* at pH 6.0 and 25 °C. Error bars represent standard deviation of the mean (± SD, n = 2).

Cd^{2+} ions uptake by living non-growing cells of G+ bacteria *K. palustris* and *M. luteus* was time (Fig. 2 and 3) and concentration (Fig. 4 and 5) dependent process. Initial rapid phase of Cd uptake followed by the slower phase was observed in both bacteria. Sequential extraction of bacterial biomass (5 mM $Ca(NO_3)_2$ and 40 mM Na_2EDTA) used for Cd cell compartmentalization indicated that the prevailing part of uptaken Cd^{2+} ions is associated with cell surface in both bacteria (Fig. 2, 3). Therefore surface complexation and electrostatic attractions played a key role in Cd removal from solution by living non-growing bacterial cells.

However, both bacteria exhibit also intracellular accumulation of Cd^{2+} ions. At initial Cd concentration of 100 µmol/L, after 4 h incubation up to 35 µmol/g (*M. luteus*) and 25 µmol/g (*K. palustris*) of Cd^{2+} ions were localized in cytoplasm. In case of *K. palustris* (Fig. 3) a slight decrease of Cd bound on cell surface from 139 ± 9 µmol/g to 113 ± 4 µmol/g and simultaneous increase of Cd in cytoplasm from 18 ± 1 µmol/g to 25 ± 4 µmol/g was observed.

Although the total removal of Cd (extracellular + intracellular sequestration) by living non-growing bacterial cells at initial Cd concentration of 100 µmol/L after 4 h incubation was higher in *K. palustris* (138 µmol/g) in comparison with *M. luteus* (100 µmol/g), *M. luteus* exhibited higher intracellular Cd accumulation. This indicates higher resistance of *M. luteus* towards Cd what is in conformity with the obtained Cd IC_{50} values (Table 1). Observed differences in uptake capacities are not surprising and can be attributed primarily to differences in cell morphology of *K. palustris* and *M.*

luteus and also to different strategies of resistance to Cd^{2+} ions. HRYNKIEWICZ *et al.* (2015) pointed out that the ability of soil bacteria to accumulate Cd^{2+} ions is strain specific and the variation within a species can exceed the variation between different species or genera.

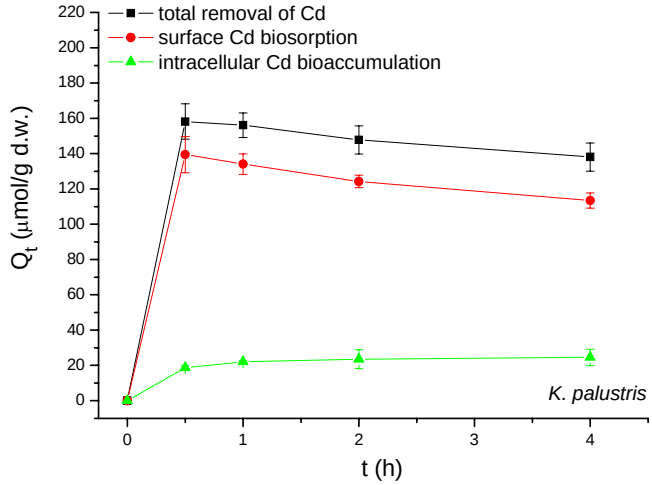

Fig. 3. Kinetics of Cd removal (C_0 = 100 µmol/L $CdCl_2$, 37.1 kBq/L $^{109}CdCl_2$) by living non-growing cells of *K. palustris* at pH 6.0 and 25 °C. Error bars represent standard deviation of the mean (± SD, n = 2).

Cd biosorption and bioaccumulation relationship were also investigated as a function of the Cd initial concentration in solution. To describe the association of Cd^{2+} ions with extracellular binding sites (biosorption) and cytoplasm (bioaccumulation) the Langmuir isotherm model (Eq. 2) was used. Results demonstrated that with increasing concentration of Cd^{2+} ions in solution extracellular binding (biosorption) of Cd increased in both bacteria (Fig. 4 and 5). Obtained curves are typical for metal biosorption by dead biomass of bacteria, fungi, algae and others (HETZER *et al.*, 2006; HRYNKIEWICZ *et al*., 2015).

M. luteus showed significantly higher uptake values at higher Cd initial concentrations (500 – 1000 µmol/L) than *K. palustris* (Fig. 4 and 5). Maximum Cd surface binding capacities $Q_{ex\ max}$ calculated from Langmuir model were 775 ± 111 µmol/g d.w. for *M. lutues* and 430 ± 37 µmol/g d.w. for *K. palustris* (Table 2). Q_{ex} values indicate that up to 85 % (*M. luteus*) and 83 % (*K. palustris*) of Cd was associated with exchangeable binding sites and/or non-covalently bound to cell surface polymers including proteins and membrane associated lipocarbohydrates of G+ bacteria. The role of functional groups in Cd binding will be discussed separately. According to literature review also Cd microprecipitation on cell surface in the form of cadmium hydroxides and phosphates can not be neglected (KOTRBA *et al*., 2010; GUIBAUD *et al*., 2006).

Intracellular accumulation of Cd^{2+} ions (Q_{in}) increased only slightly with increasing initial Cd concentration (Fig. 4 and 5). The amount of Cd in *M. luteus* cytoplasm was 2 times higher than that of *K. palustris* in the studied Cd concentration

range (100 to 1000 µmol/L). $Q_{in\ max}$ values calculated from Langmuir model were 157 ± 25 µmol/g d.w. for *M. lutues* and 74.9 ± 7.1 µmol/g d.w. for *K. palustris* (Table 2).

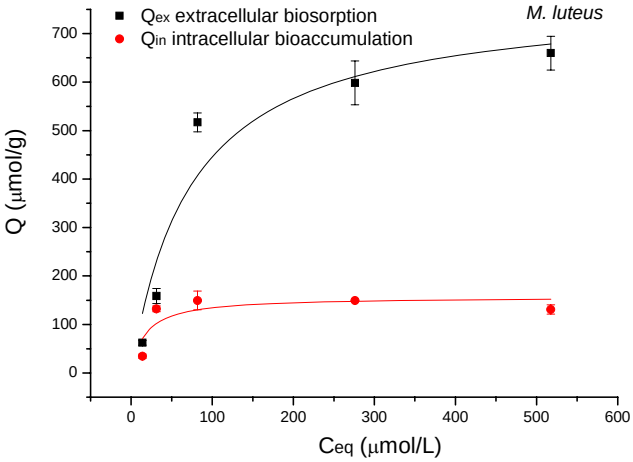

Fig. 4. Langmuir isotherms of Cd associated with cell surface and Cd localized in intracellular space of living non-growing cells of *M. luteus*. Individual points represent experimental data; curves represent the calculated values from Langmuir model. Error bars represent standard deviation of the mean (± SD, n = 2).

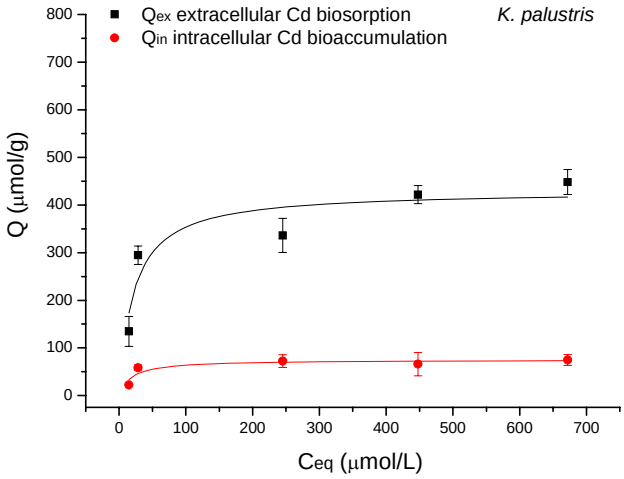

Fig. 5. Langmuir isotherms of Cd associated with cell surface and Cd localized in intracellular space of living non-growing cells of *K. palustris*. Individual points represent experimental data; curves represent the calculated values from Langmuir model. Error bars represent standard deviation of the mean (± SD, n = 2).

As has been previously reported, bacteria accumulated Cd^{2+} ions via uptake systems for essential divalent metals. E.g. in *Escherichia coli*, Cd^{2+} ions enter cells via a Zn^{2+} transport system (LADDAGA and SILVER, 1985) and in G+ bacteria (*Lactobacillus plantarum, Bacillus subtilise*) through transport systems for Mn^{2+} ions

(HAO *et al*., 1999). PABST *et al*. (2010) observed that 90 % of the initial Cd was associated with the surface of the cells of G- bacteria *Pseudomonas putida* Corvallis and *Pseudomonas putida* KT2440 and only minor part was observed in cytoplasm. In another study with G+ bacteria, HUANG *et al.* (2014) revealed that when Cd solution concentrations were less than 165 μmol/L intracellular accumulation of Cd by growing *Bacillus cereus* RC-1 was higher than surface adsorption. Above this concentration the Cd surface sorption increased significantly. Authors hypothesized that at higher Cd concentrations the efflux mechanism might be functional in order to maintain intracellular Cd below a toxic threshold. KIESLING (1997) proposed that some bacteria (*Pseudomonas, Klebsiella, Arthrobacter*) used polyphosphates localized in granules to detoxify cadmium transported into cytoplasm. However, we suppose that at lower Cd concentration the cell surface binding (biosorption) of Cd^{2+} ions could be the main detoxification mechanism in both bacteria studied. These findings are in an agreement with results obtained by HRYNKIEWICZ *et al*. (2015).

Table 2. Langmuir sorption isotherms and parameters for Cd^{2+} ions in specific cell compartments of *K. palustris* and *M. luteus* calculated using non-linear regression analysis.

Bacteria	**Compartmentalization of Cd**	Q_{max} [μmol/g]	b [L/μmol]	R^2	**% Cd associated in cell compartments**
Kocuria palustris	extracellular	430 ± 37	0.046 ± 0.020	0.860	85.2
	intracellular	74.9 ± 7.1	0.056 ± 0.027	0.818	14.8
Micrococcus luteus	extracellular	775 ± 111	0.014 ± 0.006	0.927	83,2
	intracellular	157 ± 25	0.059 ± 0.038	0.670	16.8

3.3 Cd^{2+} uptake by non-living bacteria

3.3.1 Cd^{2+} uptake kinetics

The kinetic studies were realized also using dried bacterial biomass (Fig. 6) and as expected we found that the biosorption of Cd^{2+} ions by *K. palustris* and *M. luteus* is a rapid process. At initial phase driving force is high and available high affinity binding sites on biomass are occupied. In case of *M. luteus* residual sites with lower affinity are occupied slowly during the next 2 h. A slight decrease of Cd uptake was observed in case of *K. palustris*. In both bacteria the final equilibrium was reached within 200 min and after this time there was no considerable increase until the end of experiments. *M. luteus* exhibited slightly higher Cd sorption (266 ± 3 μmol/g d.w.) in comparison with *K. palustris* (235 ± 4 μmol/g d.w.). Based on obtained results, subsequent Cd sorption experiments were realized with an equilibration time 4 h.

These findings are in agreement with other studies of Cd biosorption by bacterial surfaces. ALAM and AHMAD (2013) revealed that Cd^{2+} ions biosorption by dried biomass of Gram-positive *Exiguobacterium sp*. ZM-2 was rapid during the first 15 min

and equilibrium was reached after 120 min. Full sorption of Cd by thermophilic bacterium *Anoxybacillus flavithermus* occurred within 45 min (BURNETT *et al*., 2006). The fast rate of Cd uptake suggests that the biosorption is dependent solely on passive cadmium-sequestering processes such as electrostatic and chemical attraction between Cd^{2+} ions and the negatively charged functional groups present on the bacterial cell wall, microprecipitation and physical entrapment.

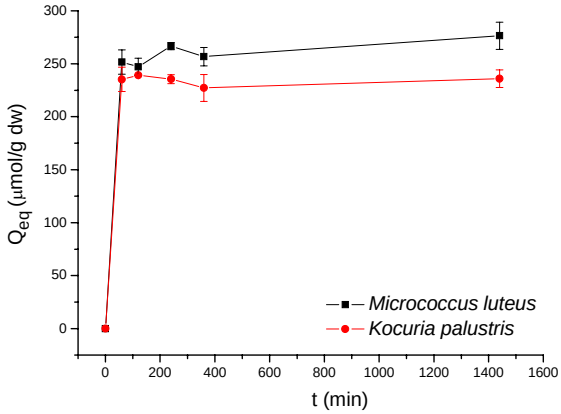

Fig 6. Kinetics of Cd (1000 µmol/L $CdCl_2$, 58.1 kBq/L ^{109}Cd) biosorption by dried biomass of *K. palustris biomass* (2.5 g/L d.w.) and *M. luteus* (2.5 g/L d.w.) at 20 °C and pH 6.0. Error bars represent standard deviation of the mean (± SD, n = 2).

3.3.2 Effect of pH

The experimental data show that biosorption increased with increasing pH and maximum uptake of Cd by both bacteria occurred at pH 7.0 (*K. palustris* 256 ± 2 µmol/g d.w.; *M. luteus* 273 ± 5 µmol/g d.w.). Slightly lower biosorption was observed from pH 4.0 to 6.0 and negligible at pH 2.0. With increasing pH, deprotonation of binding sites increased and Cd^{2+} cations are electrostatically attracted by negatively charged functional groups on bacterial cell wall. At lower pH values a strong competition between H^+ and Cd^{2+} during occupation of binding sites occurs. Moreover, extreme pH values (low and high) can damage the structure of dried bacterial biomass and therefore decrease Cd uptake. BOYANOV *et al.* (2003) using X-ray adsorption spectroscopy revealed that Cd^{2+} ions biosorption onto G+ bacterium *Bacillus subtilis* at pH 3.4 is predominated by phosphoryl ligands, whereas carboxylic ligands are the dominant binding sites in the pH range of 5.0 to 7.8. Similarly, the maximum uptake of Cd by G- bacterium *Acidiphilium symbioticum* H8 was observed at pH 6.0 (CHAKRAVARTY and BANERJEE, 2012).

However, pH affects not only binding site dissociation on bacterial surfaces, but also the solution chemistry of the cadmium. Calculation by Visual MINTEQ speciation program showed that cadmium predominantly exists as cations Cd^{2+} (~88%) and $CdCl^+$ (~10%) within pH ranging from 2.0 to 7.5 (Fig. 7). Also other cadmium ionic forms such as $CdOH^+$, Cd_2OH^{3+}, $Cd(OH)_3^-$ and $Cd(OH)_4^{2-}$ are present

in solution between pH 8.0 and 12.0. The concentration of Cd^{2+} starts to decrease at pH > 8.0 and the precipitation of Cd started at pH > 9.0.

Maximum Cd biosorption was observed at pH 7.0 when Cd^{2+} cations represent 87.5 % of total ionic forms of cadmium. However, $CdCl^{+}$ is a complex that forms under experimental conditions studied (~10%) and it is expected to adsorb onto negatively-charged functional groups too. McLEAN *et al.* (2013) confirmed the uptake of $CdCl^{+}$ complexes onto cell surface of *Pseudomonas putida*.

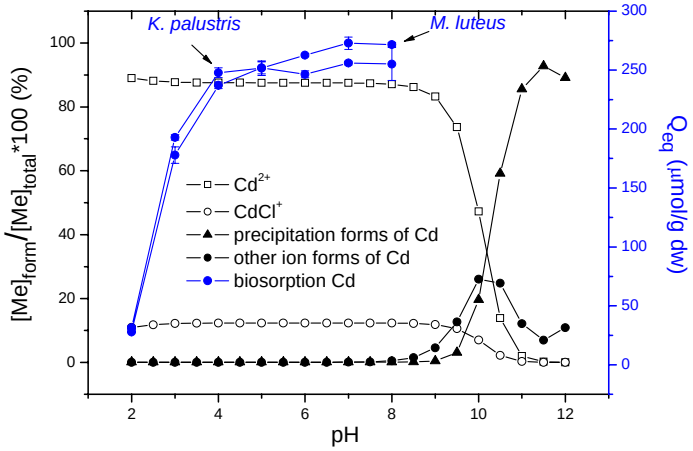

Fig. 7. Effect of pH on the biosorption of Cd (1000 μmol/L, 43.8 kBq/L $^{109}CdCl_2$) by dried biomass of *K. plaustris* (2.5 g/L, dw) and *M. luteus* (2.5 g/L, dw) and Cd speciation in solution. Error bars represent standard deviation (SD) of the mean (n = 2). Theoretical Cd speciation was calculated using Visual MINTEQ version 3.0 with initial conditions: 1000 μmol/L $CdCl_2$, T = 20°C, pCO_2 = 38.5 Pa.

3.3.3 Equilibrium Cd^{2+} biosorption

Generally known Langmuir (Eq 2) and Freundlich (Eq 3) isotherms were fitted to the equilibrium data for Cd^{2+} ions biosorption by non-living biomass of *K. palustris* and *M. luteus*. Isotherm curves and parameters of the models determined from the experimental data using non-linear regression analysis are reported in Fig. 8A, B and Table 3. The Langmuir isotherm fits the data of Cd^{2+} ions biosorption by both bacteria better than the Freundlich isotherm, as is demonstrated by higher values of the coefficient of determination (R^2), by the lower of the sum of squares (*RSS*) values obtained and by the more homogeneous standard deviation of each observed parameter (Table 3). Also other authors found that the sorption of Cd^{2+} ions by *Pseudoalteromonas* sp. SCSE709-6 (ZHOU *et al*., 2014), *Bacillus cereus* RC-1 (HUANG *et al*., 2013), *Acidiphilium symbioticum* H8 (CHAKRAVARTY and BANERJEE, 2012) and activated sludge (REMENÁROVÁ *et al*., 2012) was well described using the Langmuir isotherm.

The maximum sorption capacity Q_{max} of *M. luteus* obtained from the Langmuir isotherm for Cd^{2+} was 444 ± 15 μmol/g. A lower value of Q_{max} was observed in the case of *K. palustris* biomass, i.e. 381 ± 1 μmol/g. As was mentioned in the case of

living bacteria, observed differences in uptake capacities can be attributed to differences in cell morphology of *K. palustris* and *M. luteus.* The affinity constant *b* of the isotherms corresponds to the initial gradient, which indicates the bacterial biomass affinity at low concentrations of Cd ions. A higher initial gradient corresponds to a higher affinity constant *b* (SHENG *et al*., 2007). From Fig. 8A and 8B it is evident that both isotherms have similar behaviour at lower equilibrium concentrations. The difference in the *b* values 0.0042 ± 0.0005 L/μmol (*M. luteus*) and 0.0083 ± 0.0001 L/μmol (*K. palustris*), indicates higher affinity of *K. palustris* for Cd ions, although *M. luteus* exhibited higher maximal capacity (Table 3).

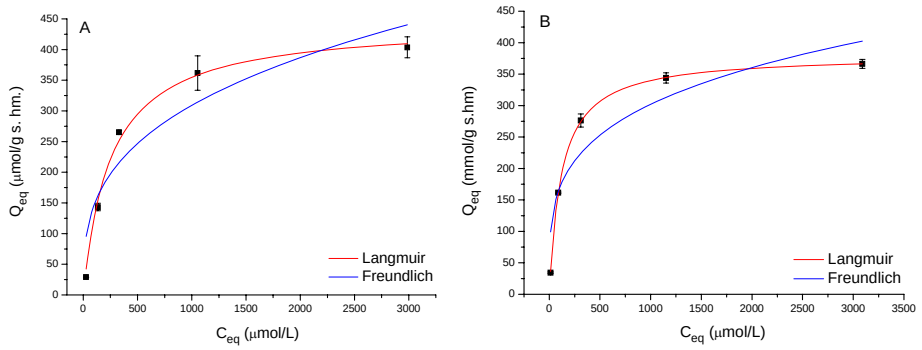

Fig. 8. Adsorption isotherm of Cd^{2+} by dried biomass of *M. luteus* and *K. palustris* (2.5 g/L) at 20 °C and pH 6.0 according to Langmuir and Freundlich with experimental points. Error bars represent the standard deviation of the mean (± SD, n = 2).

Table 3. Langmuir and Freundlich parameters for the biosorption of Cd^{2+} ions by dried biomass of *M. luteus* and *K. palustris* obtained by non-linear regression analysis.

Bacteria	Langmuir				Freundlich			
	Q_{max} [μmol/g]	***b*** [L/μmol]	R^2	***RSS***	***K*** [L/g]	***1/n***	R^2	***RSS***
M. luteus	444 ± 15	0.0042 ± 0.0005	**0.995**	**523**	33.0 ± 20.25	0.32 ± 0.08	**0.888**	**10747**
K. palustris	381 ± 1	0.0083 ± 0.0001	**0.999**	**6.8**	52.0 ± 26.0	0.25 ± 0.07	**0.880**	**9153**

Despite the fact that the Langmuir isotherm offers no insights into the biosorption mechanism (LIU and LIU, 2008) it is still a convenient tool for comparing data on a quantitative basis (Q_{max}, *b*). Obtained results show that the maximum specific uptake capacities Q_{max} of Cd were higher for living non-growing biomass (Table 2) in comparison with non-living (dried) biomass (Table 3) of both bacteria. Similar to our findings, ALAM and AHMAD (2013) demonstrated higher efficiency of non-growing biomass of *Exiguobacterium* sp. ZM-2 to adsorb Cd^{2+} ions than dried biomass. Authors pointed out that some part of Cd^{2+} ions was transported into cytoplasm of non-growing cells what was also confirmed in our study (Fig. 4 and 5). Contrary,

HUANG *et al.* (2013) based on Q_{max} and b values inspection revealed that dead biomass of *Bacillus cereus* RC-1 was more efficient in adsorbing Cd^{2+} ions than live biomass.

3.4 The role of functional groups of cell components in Cd^{2+} binding

FTIR analysis was performed to identify the surface nature of dried *K. palustris* and *M. luteus*, as well as to identify major functional groups and to confirm their participation in Cd uptake. Obtained spectra reflect a complex character of both bacterial surfaces and illustrate significant changes in transmittance of characteristic peaks after Cd biosorption (Fig. 9 and 10). Bands in the FTIR spectrum were assigned to various groups according to wave numbers (Table 4) as reported in literature (HUANG *et al*., 2014; ZHOU *et al*., 2014; GARIP *et al*., 2009).

Table 4. Main functional groups of *K. palustris* and *M. luteus* with corresponding wave numbers obtained using FTIR analysis.

KP	**KP-Cd**	**ML**	**ML-Cd**	**Vibration type**	**Functional type**
wavenumber (cm^{-1})		wavenumber (cm^{-1})			
3 325	3 331	3 360	3 377	stretching vibration of OH	-OH of polysaccharides and proteins
2 929	2 929	2 924	2 922	asymetric vibration of $–CH_2$	lipids
1 653	1 651	1 679	1 651	strong vibration of C=O and C-N (primary amide)	proteins (peptidic bond)
1 541	1 537	1 539	1 537	stretching vibration of C-N and deformation vibration of N-H (secondary amide)	proteins (peptidic bond)
1 379	1 379	1 392	1 384	C=O symetric stretching of COO^-	carboxylates and carboxylic acids
1 236	1 232	1 238	1 236	asymetric vibration of PO_2^-	phospholipids
1 060	1 064	1 066	1 060	symetric vibration of PO_2^-	phospholipids

KP – unloaded *K. palustris*; ML – unloaded *M. luteus*; KP-Cd – Cd loaded *K. palustris*, ML-Cd – Cd loaded *M. luteus.*

FTIR spectra of unloaded and Cd loaded *K. palustris* biomass is shown on Fig. 9. It is obvious that asymetric vibration of PO_2^- group (phospholipids) at 1236 cm^{-1} and symetric vibration of PO_2^- group at 1060 cm^{-1} were shifted after Cd biosorption. Although, significant shift of absorption band corresponding to COO^- (1 379 cm^{-1}) was not detect, changes in peak intensity was observed after Cd treatment. The reason is probably the presence of Ca and Mg bound with carboxyl and phosphoryl groups of *K. palustris*, which have been replaced by Cd^{2+} ions in the process of ion exchange. We suppose that carboxylate ions may coordinate to Cd^{2+} ions as chelating complexes.

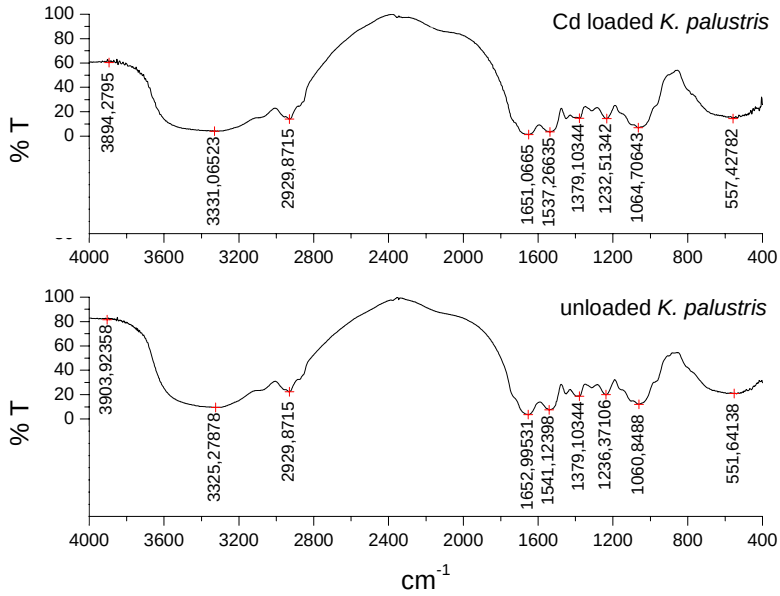

Fig. 9. FTIR spectrum of *K. palustris* biomass before and after Cd sorption.

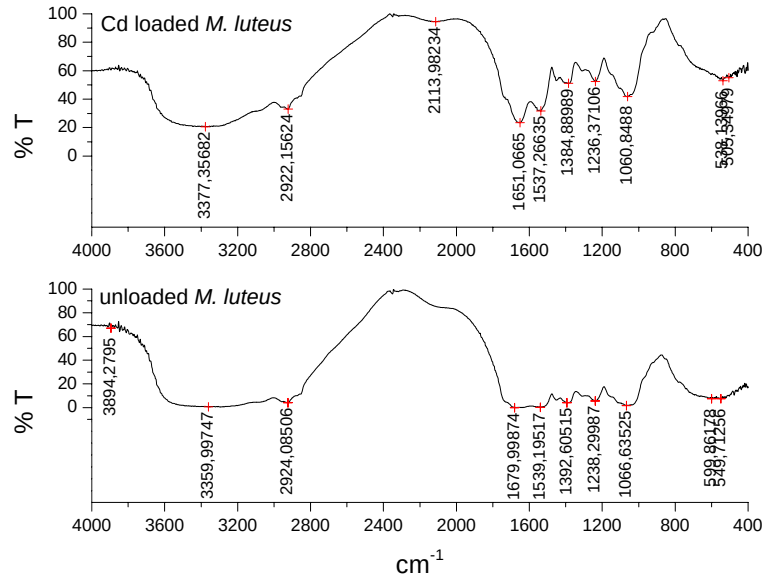

Fig. 10. FTIR spectrum of *M. luteus* biomass before and after Cd sorption.

The main differences between spectra of unloaded and Cd loaded *M. luteus* biomass are associated with the primary amide (C=O) vibrations and C=O symetric

stretching of COO^-. Evident shifts of absorption band from 1651 cm^{-1} to 1679 cm^{-1} and 1384 cm^{-1} to 1392 cm^{-1} after Cd uptake were observed (Table 4, Fig. 10). As seen from Fig. 10, the intensity of bands at 1 655, 1 537 and 1 384 cm^{-1} decreased considerably after Cd biosorption. Beside carboxylate ions also other functional groups such as amino and hydroxyl may contribute to Cd binding by cell surfaces. GIRAULT *et al.* (1997) observed strong Cd binding to membrane phospholipids. Using ^{113}Cd and ^{31}P-NMR confirmed that Cd interactions with membrane phospholipids are electrostatic in nature and the phosphate moiety is proposed as a binding site. Although there are differences in Cd sorption capacities of *K. palustris* and *M. luteus* we expected that the functional groups of teichoic and teichuronic acids that are characteristic for G+ bacteria mediated Cd uptake onto cell surface by both live and dead bacterial biomass.

4. Conclusions

Using radioindicator method with ^{109}Cd we confirmed that living non-growing cells of G+ bacteria *K. palustris* and *M. luteus* effectively taken up Cd ions. Up to 85 % (*M. luteus*) and 83 % (*K. palustris*) of Cd was associated with exchangeable binding sites and/or non-covalently bound to cell surface polymers. Intracellular accumulation of Cd^{2+} ions increased only slightly with increasing initial Cd concentration. The maximum specific Cd uptake capacities Q_{max} obtained from the Langmuir isotherm were higher for living non-growing biomass in comparison with non-living (dried) biomass of both bacteria. The biosorption of Cd^{2+} ions by non-living biomass of *K. palustris* and *M. luteus* is strongly affected by pH and initial Cd concentration. The maximum sorption capacities Q_{max} were 444 ± 15 μmol/g for *M. luteus* and 381 ± 1 μmol/g for *K. palustris*. FTIR analysis indicates that beside carboxylate ions also other functional groups such as amino and phosphate contribute to Cd binding by bacterial cell surfaces. The present results suggest that beside dead bacterial biomass also living non-growing bacterial cells may be applied for biosorption purposes especially in low concentrations of Cd in water.

References

ADAM, V., CHUDOBOVA, D., TRNEJOVA, K., CIHALOVA, K., KRIZKOVA, S., GURAN, R., KOMINKOVA, M., ZUREK, M., KREMPLOVA, M., JIMENEZ, A.M.J., KONECNA, M., HYNEK, D., PEKARIK, V., KIZEK, R.: An effect of cadmium and lead ions for methallothionein (MT-3) revealed by electrochemistry. Electrochim. Acta, 140, 2014, 11-19.

ALAM, M.Z., AHMAD, S.: Multi-metal biosorption and bioaccumulation by *Exiguobacterium* sp. ZM-2. Ann. Microbiol., 63, 2013, 1137-1146.

BESTAWY, E.E., HELMY, S., HUSSEIN, H., FAHNY, M., AMER, R.: Bioremediation of heavy metal-contaminated effluent using optimized activated sludge bacteria. Appl. Water. Sci., 3, 2013, 181-192.

BURNET, P.G.G., DAUGHNEY, CH.J., PEAK, D.: Cd adsorption onto *Anoxybacillus flavithermus*: Surface complexation modelling and spectroscopic investigations. Geochim. Cosmochim. Acta, 70, 2006, 5253-5269.

BOYANOV, M.I., KELLY, S. D., KEMNER, K. M., BUNKER, B. A., FEIN, J. B., FOWLE, D. A.: Adsorption of cadmium to *Bacillus subtilis* bacterial cell walls: a pH-dependent X-ray absorption fine structure spectroscopy study. Geochim. Cosmochim. Acta, 67, 2003, 3299–3311.

GARIP, S., GOZEN, A.C., SEVERCAN, F.: Use of Fourier transform infrared spectroscopy for rapid comparative analysis of *Bacillus* and *Micrococcus* isolates. Food Chem., 113, 2009, 1301-1307.

GIRAULT, L., BOUDOU, A., DUFOURC, E.J.: 113Cd-, 31P-NMR and fluorescence polarization studies of cadmium(II) interactions with phospholipids in model membranes. Biochim. Biophys. Acta, 1414, 1998, 140-154.

GUIBAUD, G., HULLEBUSCH, E., BORDAS, F.: Lead and cadmium biosorption by extracellular polymeric substances (EPS) extracted from activated sludges: pH-sorption edge tests and mathematical equilibrium modelling. Chemosphere, 64, 2006, 1955-1962.

GUSTAFFSON, J.P. Visual-MINTEQ, version 3.0. (2004), http://vminteq.lwr.kth.se/download/

HAO, Z., REISKE, H., WILSON, D.: Characterization of cadmium uptake in *Lactobacillus plantarum* and isolation of cadmium and manganese uptake mutants. Appl. Environ. Microbiol., 65, 1999, 4741-4745.

HETZER, A., DAUGHNEY, CH.J., MORGAN, H.W.: Cadmium ion biosorption by the thermophilic bacteria *Geobacillus stearothermophilus* and *G. thermocatenulatus*. Appl. Environ. Microbiol., 72, 2006, 4020-4027.

HRYNKIEWICZ, K., ZLOCH, M., KOWALKOWSKI, T., BAUM, CH., NIEDOJADLO, K., BUSZEWSKI, B.: Strain-specific bioaccumulation and intracellular distribution of Cd^{2+} in bacteria isolated from the rhizosphere, ectomycorrhizae, and fruitbodies of ectomycorrhizal fungi. Environ. Sci. Pollut. Res., 4, 2015, 3055-3067.

HUANG, F., DANG, Z., GUO, CH.L., LU, G.N., GU, R.R., LIU, H.J., ZHANG, H.: Biosorption of Cd(II) by live and dead cells of *Bacillus cereus* RC-1 isolated from cadmium-contaminated soil. Colloids Surf. B Biointerfaces, 107, 2013, 11-18.

HUANG, F., GUO, CH.L., LU, G.N., YI, X.Y., ZHU, L.D., DANG, Z.: bioaccumulation characterization of cadmium by growing *Bacillus cereus* RC-1 and its mechanism. Chemosphere, 109, 2014, 134-142.

CHAKRAVARTY, R., BANERJEE, P.C.: Mechanism of cadmium binding on the cell wall of an acidophilic bacterium. Bioresour. Technol., 108, 2012, 176-183.

CHOJNACKA, K.: Bioaccumulation of Cr(III) ions by Blue-Green alga *Spirulina sp.* Part I. A Comparison with Biosorption. Am. J. Agric. Biol. Sci., 4, 2007, 218-223.

CHOJNACKA, K.: Biosorption and bioaccumulation – the prospects and practical applications. Environ. Int., 36, 2010, 299-307.

KADUKOVA, J., VIRCIKOVA, E.: Comparison of differences between copper bioaccumulation and biosorption. Environ. Int., 31, 2005, 227-232.

KIESLING, J.D.: Regulation of intracellular toxic metals and other cations by hydrolysis of polyphosphate. Ann. N. Y. Acad. Sci., 829, 1997, 242-249.

KOTRBA, P., RUML, T.: Surface display of metal fixation motifs of bacterial Pi-Type ATPases specifically promotes biosorption of Pb^{2+} by *Saccharomyces cerevisiae.* Appl. Environ. Microbiol., 76, 2010, 2615-2622.

LADDAGA, R.A, SILVER, S.: Cadmium uptake in *Escherichia coli* K-12. J. Bacteriol., 162, 1985, 1100–1105.

LIU, Y., LIU, Y.J.: Biosorption isotherms, kinetics and thermodynamics. Sep. Purif. Technol., 61, 2008, 229-242.

McLEAN, J.E., PABST, M.W., MILLER, C.D., DIMKPA, C.O., ANDERSON, A.J.: Effect of complexing ligands on the surface adsorption, internalization, and bioresponse of copper and cadmium in a soil bacterium, *Pseudomonas putida*. Chemosphere, 91, 2013, 374-382.

PABST, W.M., MILLER, CH.D., DIMKPA, CH., ANDERSON, A.J., McLEAN, J.E.: Defining the surface adsorption and internalization of copper and cadmium in a soil bacterium, *Pseudomonas putida*. Chemosphere, 81, 2010, 904-910.

REMENAROVA, L., PIPISKA, M., HORNIK, M., ROZLOZNIK, M., AUGUSTIN, J., LESNY, J.: Biosorption of cadmium and zinc by activated sludge from single and binary solutions: Mechanism, equlibrium and experimental design study. J. Taiwan Inst. Chem. Eng., 43, 2012, 433-443.

SHENG, P.X., TING, Y.P., CHEN, J.P.: Biosorption of heavy metal ions (Pb, Cu, and Cd) from aqueous solutions by marine alga *Sargassum sp.* in single- and multiple-metal systems. Ind. Eng. Chem. Res., 46, 2007, 2438-2444.

SINGH, S.N, TRIPATHI, R.D.: Bioremediation of organic and metal Co-contaminated environments: Effects of metals, toxicity, speciation, and bioavailability on biodegradation In: Environmental bioremediation Technologies. Berlin, Heidelberg: Springer-Verlag; 2007.

TISAKOVA, L., PIPISKA, M., GODANY, A., HORNIK, M., VIDOVA, B., AUGUSTIN, J.: Bioaccumulation of ^{137}Cs and ^{60}Co by bacteria isolated from spent nuclear pools. J. Radioanal. Nucl. Chem., 295, 2013, 737-748.

URIK, M., KRAMAROVA, Z., SEVC, J., CERNANSKY, S., KALIS, M., MEDVED, J., LITTERA, P., KOLENCIK, M., GARDOSOVA, K.: Biosorption and bioaccumulation of thallium(I) and its effect on growth of *Neosartorya fischeri* strain. Pol. J. Environ. Stud., 19, 2010, 457-460.

VARGAS-GARCIA, M.C., LOPEZ, M.J., SUAREZ-ESTRELLA, F., MORENO, J.: Compost as a source of microbial isolates for the bioremediation of heavy metals: *in vitro* selection. Sci. Total Environ., 431, 2012, 62-67.

ZHOU, W., DONGSHENG, L., ZHANG, H., KONG, W., ZHANG, Y.: Bioremoval and recovery of Cd(II) by *Pseudoalteromonas* sp. SCSE709-6: Comparative study on growing and grown cells. Bioresour. Technol., 165, 2014, 145-151.